6710 *Macromolecules* **2009**, *42*, 6710–6715
DOI: 10.1021/ma901089s

Macromolecules
ARTICLE

PVPylated Poly(alanine) as a New Thermogelling Polymer

Jin Ok Han, Min Kyung Joo, Ji Hye Jang, Min Hee Park, and Byeongmoon Jeong*

Department of Chemistry and Nano Science, Department of Bioinspired Science, Ewha Womans University, Daehyun-Dong, Seodaemun-Ku, Seoul, 120-750, Korea

Received May 19, 2009; Revised Manuscript Received July 16, 2009

ABSTRACT: In order to investigate poly(*N*-vinyl pyrrolidone) as an alternative to poly(ethylene glycol) in preparing a biomedical polymer, we synthesized a series of reverse thermogelling poly(*N*-vinyl pyrrolidone-*b*-alanine) (PVP-PA). The amphiphilic polymers consisting of the hydrophilic PVP block and the hydrophobic PA block formed micelles in water and the micelles aggregated as the temperature increased. FTIR spectroscopy, circular dichrosim spectroscopy, and ^{13}C NMR spectroscopy showed that the aggregation behavior accompanied a change in PA conformation as well as a decrease in the molecular motion of PVP-PA. The sol-to-gel transition temperature decreased as the PA block length increased, PVP block length decreased, and L-alanine/DL-alanine ratio of PA increased. This paper suggests that PVP can be a promising alternative to poly(ethylene glycol) in designing a reverse thermogelling biomaterial.

Introduction

Poly(*N*-vinyl pyrrolidone) (PVP) was used as a plasma expander during World War II under the trade name of Periston or Kollidon. However, the storage of the nonbiodegradable PVP with a high molecular weight ($M_w > 30\,000$) in the organism raised a significant question about its use as a plasma expander.[1] The low molecular weight PVP and its copolymers have been investigated for drug conjugation,[2] liposomes,[3] micelles,[4] gene carriers,[5] and nanoparticles.[6] In particular, several examples below suggest the importance of PVP as an alternative to poly(ethylene glycol) (PEG). PVP ($M_n \sim 6000$ Da) conjugated tumor necrosis factor-α (TNF-α) showed a higher antitumor activity and prolonged plasma half-life than TNF-α and PEG conjugated TNF-α.[2] PVPylated liposome prepared from PVP conjugated lipids exhibited a prolonged circulation time after intravenous injection.[3] Poly(*N*-vinyl pyrrolidone-*b*-DL-lactide) (PVP-PDLLA) nanoparticles, where the molecular weight of PVP was in the range 2500−4800 Da, exhibited a greater extent of opsonization and was swiftly taken up by Kuffer cells, and thus had a shorter plasma circulation time than the PEG-PDLLA system.[6] In addition, PVP showed excellent cryoprotective properties and was used as a cryoprotectant for cells and lyoprotectant for proteins.[7,8]

As a minimally invasive injectable system, reverse thermal gelling biodegradable polymer aqueous solutions have been extensively sought during the past decade.[9−11] They are low viscous aqueous solutions at a low temperature and undergo sol-to-gel transition as the temperature increases. The in situ formed hydrogel depot containing pharmaceutical agents acts as a sustained release system of the incorporated drug. The reverse thermal gelation comes from the delicate balance between hydrophilicity and hydrophobicity of a polymer. Polyesters, polysaccharides, polyphosphazenes, poly(*N*-(2-hydroxypropyl) methacrylamide-oligolactate)s, polycarbonates, polycyanoacrylates, polypeptides, etc have been used as a biodegradable hydrophobic block, whereas poly(ethylene glycol) has been used as a hydrophilic block in most cases.[12−19]

Here, we are reporting PVP conjugated polyalanine, so-called PVPylated polyalanine (PVP-PA), as a new thermogelling polymer. The sol-to-gel transition mechanism was investigated by various instruments. The structure−property relationship of sol-to-gel transition was investigated by varying PVP molecular weight, PA molecular weight, and the ratio of L-alanine to DL-alanine.

*Corresponding author. E-mail: bjeong@ewha.ac.kr.

Experimental Section

Materials. *N*-vinyl pyrrolidone, 2-aminoethanethiol, azobis(isobutyronitrile) (AIBN), 2-anilinonaphthalene, and benzene were used as received from Aldrich. *N*-Carboxy anhydrides of L-alanine and *N*-carboxy anhydrides of DL-alanine (M & H Laboratory, Korea) were used as received. Toluene was dried over sodium before use. Chloroform and *N*,*N*-dimethylformamide (anhydrous) were treated with anhydrous magnesium sulfate before use.

Synthesis. Amine-terminated PVP was synthesized by free-radical polymerization of *N*-vinyl pyrrolidone in the presence of 2-aminoethanethiol.[4c−e] For example, to prepare the PVP-II in Table 1, *N*-vinyl pyrrolidone (106.6 mL; 1.0 mol), benzene (250 mL), and 2-aminoethanethiol (5.01 mL; 0.049 mol) were added in a round-bottom flask. Nitrogen was purged for 1 h to eliminate the oxygen in the reaction system. AIBN (6.08 g; 0.037 mol) was added under nitrogen flow, and the polymerization was carried out for 24 h at 70 °C. The reaction mixtures were precipitated into diethyl ether. The residual solvent in the precipitate was eliminated under vacuum.

PVP-PA (PIII) was prepared by ring-opening polymerization of the *N*-carboxy anhydrides of L-alanine and *N*-carboxy anhydrides of DL-alanine in the presence of amine-terminated PVP (PVP-II).[20,21] PVP (PVP-II) (15.0 g ; 0.012 mol; MW 1240 Da) was dissolved in toluene (100 mL) and the residual water was removed by azeotropic distillation to a final volume of about 20 mL. Anhydrous chloroform/dimethylformamide (65 mL; 12/1 v/v), *N*-carboxy anhydrides of L-alanine (2.61 g; 0.0227 mol), and *N*-carboxy anhydrides of DL-alanine (6.09 g; 0.0530 mol) were added to the reaction flask and were stirred at 40 °C for 24 h. The reaction mixtures were precipitated into diethyl ether, and the residual solvent in the precipitate was eliminated under vacuum. The polymer was further purified by dialysis (cutoff molecular weight of membrane was 1000 Da) for 24 h. The remaining polymer aqueous solution in the dialysis bag was freeze-dried to produce the white powder form of the polymer.

 Published on Web 07/27/2009

Table 1. List of Polymers Studied

polymer	PVP-PA[a]	PVP-PA[b]	L/DL[c]	M_n[a]	M_w/M_n[a]
PVP-I	970			970	1.2
PVP-II	1240			1240	1.1
PI	970−510	970−650	30/70	1480	1.1
PII	1240−350	1240−510	30/70	1590	1.1
PIII	1240−580	1240−720	30/70	1820	1.1
PIV	1240−880	1240−950	30/70	2120	1.2
PV	1240−540	1240−700	20/80	1780	1.1
PVI	1240−520	1240−660	40/60	1760	1.1

[a] Determined by MALDI−TOF mass spectra. [b] Determined by ^{1}H NMR (CF_3COOD) spectra. The ratio of the number of repeating unit of *N*-vinyl pyrrolidone (*m*) to that of alanine (*n*) was determined by the equation $A_{4.7-4.9}/A_{2.6-3.0} = n/(2m+4)$. The $A_{4.7-4.9}$ and $A_{2.6-3.0}$ are the integration area of ^{1}H NMR at 4.7−4.9 ppm and 2.6−3.0 ppm, respectively. The ^{1}H NMR spectra of PVP-PA are shown in Figure S1. The M_n of the molecular weight of PVP was given by MALDI−TOF mass spectra. [c] The L-alanine/DL-alanine ratio of PVP-PA was determined by the monomer feed, assuming that the reactivity of *N*-carboxy anhydride of L-alanine is the same as the *N*-carboxy anhydride of DL-alanine.

The yield was about 60%. Other polymers with different composition and block length were similarly prepared. Table 1 summarizes the list of polymers studied in this paper.

MALDI−TOF Mass Spectroscopy. The matrix assisted laser desorption and ionization-time-of-flight (MALDI−TOF) mass spectra of PVP and PVP-PA were obtained by a mass spectrometer (Voyager-DE STR; Applied Biosystems, Foster, CA) equipped with a nitrogen laser emitting pulsed UV light at 337 nm and operated at an acceleration voltage of 20 kV in the reflector mode. Then, 5 μL of a polymer matrix solution (1 mg/mL) consisting of α-cyano-4-hydroxycinnamic acid solution (4 mg/mL) of 60/40 (v/v) acetonitrile/water mixture containing 0.1% trifluoroacetic acid was deposited on the MALDI−TOF plate and was air-dried at room temperature. All measurements were performed in a positive ion mode.

^{1}H and ^{13}C NMR Spectroscopy. ^{1}H NMR spectra of the PVP-PA (in CF_3COOD) (500 MHz NMR spectrometer; Varian) were used to determine the composition of the polymer. ^{1}H NMR spectra of PVP-PA (PIII) (in D_2O) were compared with the spectra in CF_3COOD at 20 °C to prove the core−shell structure of the polymer in water.[22,23] ^{13}C NMR spectral changes of the PVP-PA (PIII; 12.0 wt % in D_2O) were investigated as a function of temperature. The solution temperature was equilibrated for 20 min at each temperature.

Phase Diagram. The sol−gel transition of the polymer aqueous solution was investigated by the test tube inverting method.[24] The aqueous polymer solution (1.0 mL) was added into a vial with an inner diameter of 11 mm. The transition temperature was determined by flow− (sol−) nonflow (gel) criterion with a temperature increment of 1 °C each step. Each data point is an average of three measurements.

Dynamic Mechanical Analysis. Changes in modulus of the polymer aqueous solutions were investigated by dynamic rheometry (Thermo Haake, Rheometer RS 1).[25] The aqueous polymer solution was placed between parallel plates of 25 mm diameter and a gap of 0.5 mm. To minimize the water evaporation during experiment, the plates was enclosed in a water saturated chamber. The data were collected under a controlled stress (4.0 dyn/cm^2) and a frequency of 1.0 rad/s. The heating rate was 0.5 °C/min.

Fluorescence Spectroscopy. Critical micelle concentration of PVP-PA (PIII) was investigated by fluorescence spectroscopy (RF5301, Shimadzu)) at 20 °C. 2-Anilinonaphthalene solution in methanol (10 μL at 0.01 mM) was injected into a polymer aqueous solution (1.0 mL) in a polymer concentration range of 1.0×10^{-4} to 5.0×10^{-1} wt %. The excitation wavelength was 309 nm. The fluorescence spectra of the solution were recorded from 350 to 600 nm. The band position was plotted against the polymer concentration, and the crossing point of the two extrapolated lines was defined as the critical micelle concentration.[26]

Scheme 1. Synthetic Scheme of PVP-PA

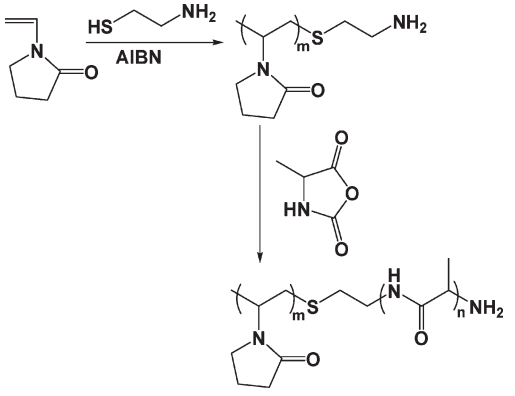

Transmission Electron Microscopy. The PVP-PA (PIII) aqueous solution (0.05 wt %, 10 μL) was placed on the carbon grid and the excess solution was blotted with filter paper. The grids were air-dried at 20 °C for 24 h. The microscopic image was obtained by JEM-2100F (JEOL) with an accelerating voltage of 200 kV.

Dynamic Light Scattering. Apparent size of PVP-PA (PIII) aggregates in water (0.05 wt %) was studied by a dynamic light scattering instrument (ALV 5000-60x0) as a function of temperature. The aqueous solution was equilibrated for 20 min at each temperature. A YAG DPSS-200 laser (Langen, Germany) operating at 532 nm was used as a light source. Measurements of scattered light were made at an angle of 90° to the incident beam. The results of dynamic light scattering were analyzed by the regularized CONTIN method. The decay rate distributions were transformed to an apparent diffusion coefficient. From the diffusion coefficient, the apparent hydrodynamic size of a polymer aggregate can be obtained by the Stokes−Einstein equation.

FTIR Spectroscopy. FTIR spectra (FTIR spectrophotometer FTS-800; Varian) of the PVP-PA (PIII) aqueous solution (12.0 wt % in D_2O) were investigated as a function of temperature in the range 10−50 °C by an increment of 5 °C each step. The resolution was 2.0 cm^{-1}. The aqueous solution was equilibrated for 20 min at each temperature. Deconvolution of the amide peak was done in the spectral range 1600−1700 cm^{-1}. The deconvoluted spectra were fitted with the XPSPEAK41 program.

Circular Dichroism (CD) Spectroscopy. Ellipticity of the PVP-PA (PIII) aqueous solution was obtained by the circular dichroism instrument (J-810, JASCO) as a function of concentration at a fixed temperature of 20 °C in a polymer concentration range of 1.0×10^{-4} to 5.0×10^{-1} wt %. In addition, ellipticity of the PVP-PA (PIII) aqueous solution was obtained as a function of temperature at a fixed concentration of 0.05 wt % in the range 10−50 °C by an increment of 5 °C each step. The aqueous solution was equilibrated for 20 min at each temperature.

Results and Discussion

The synthesis procedure of the PVP-PA is shown in Scheme 1. First, amine-terminated PVP was synthesized by free radical polymerization of *N*-vinyl pyrrolidone in the presence of 2-aminoethanethiol.[4c−e] The transfer of radicals generated from AIBN to 2-aminoethanethiol produces the thioradicals that polymerize *N*-vinyl pyrrolidone to amine-terminated PVP. Then, the *N*-carboxy anhydrides of alanine were polymerized on the amine-terminated PVP to prepare the PVP-PA.[20,21]

The MALDI−TOF mass spectra of the PVP and PVP-PA gave the unimodal distribution of the polymer (Figure 1). The molecular weight of the polymer determined by MALDI−TOF mass spectra is an absolute molecular weight. The molecular weight of PVP was less than 3,000 Da to facilitate the rapid

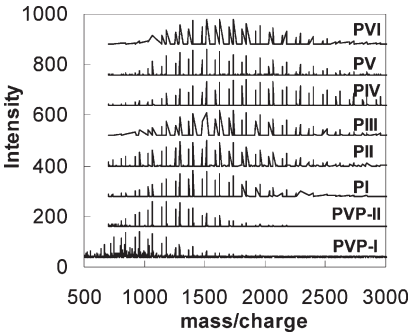

Figure 1. MALDI−TOF mass spectra of PVP and PVP-PA.

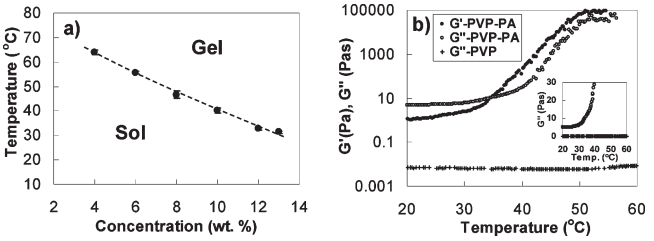

Figure 2. (a) Phase diagram of the PVP-PA (PIII) aqueous solutions determined by the test tube inverting method ($n = 3$). (b) Changes in storage modulus (G') and loss modulus (G'') of the PVP-PA (PIII) aqueous solutions (12.0 wt %) as a function of temperature. G'' of PVP aqueous solution (12.0 wt %) is shown as a reference. G' of the PVP is less than a tenth of G'' over the temperature range studied (data not shown). The data were collected with a heating rate of 0.5 °C min^{-1} and a frequency of 1.0 rad/s.

clearance by the kidney when applied in the in vivo system.[1] The molecular weight of PVP-PA was also calculated by ^{1}H NMR spectra (CF_3COOD) (Supporting Information: Figure S1). The methine peak of PA at 4.7−4.9 ppm (−NHCO***CH***(CH_3)−) and the methylene peak of PVP at 2.6−3.0 ppm (−NCH_2CH_2-***CH_2***CO− in the pyrrolidone ring) were used to calculate the composition of the PVP-PA block copolymer.[4,4c,27] The composition of L-alanine and DL-alanine was given by the feed ratio during the polymerization by assuming the same reactivity of the *N*-carboxy anhydride of L-alanine and the *N*-carboxy anhydride of DL-alanine. Table 1 lists the polymers discussed in this paper. The differences in molecular weight determined by ^{1}H NMR spectra and MALDI−TOF mass spectra might come from the phase error in the integration of the ^{1}H NMR spectra. However, the trends were well correlated with each other. The molecular weights and the molecular weight distributions of the PVP-PA were in a range of 1400−2200 Da and 1.1−1.2, respectively.

PVP-PA aqueous solutions underwent sol-to-gel transition as the temperature increased. The phase diagram of PVP-PA (PIII) aqueous solution determined by the test tube inverting method is shown in Figure 2a. As the polymer concentration increased from 4 to 13 wt % the sol-to-gel transition temperature decreased from 64 to 30 °C. Below 4.0 wt %, an increase in viscosity was observed, however, the solution was not rigid enough to stop the mass flow at high temperature. Above 14.0 wt %, the polymer aqueous solutions existed as a gel phase and sol−gel transition was not observed in a temperature range of 10 - 80 °C. The sol-to-gel transition of the PVP-PA aqueous solution involved a significant increase in the storage modulus (G') and loss modulus (G''). The crossing of the G' over G'' suggests that the elastic component dominates the viscous component at or above the sol-to-gel transition temperature. On the other hand, there is no significant change in G' and G'' of the PVP aqueous solution and G'' is larger than G' over the temperature range studied (Figure 2b).

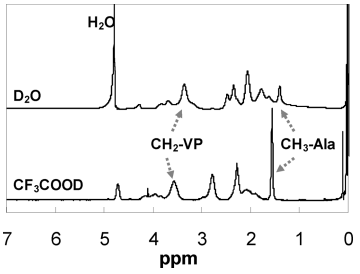

Figure 3. Comparison of ^{1}H NMR spectra of PVP-PA (PIII) in D_2O and in CF_3COOD.

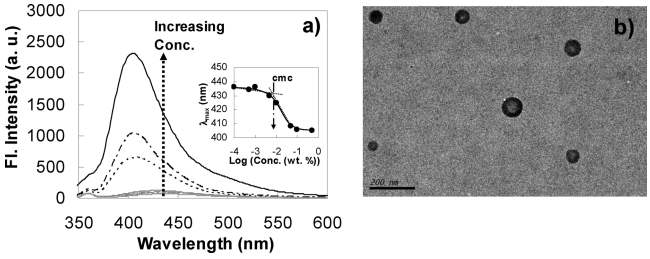

Figure 4. (a) Determination of critical micelle concentration (CMC) of the PVP-PA (PIII) in water at 20 °C by fluorescence dye (2-anilinonaphthalene). The polymer concentration varied over 1.0×10^{-4} to 5.0×10^{-1} wt % at a fixed dye concentration of 0.1 μM. (b) Transmission electron microscopy image of the PVP-PA (PIII) developed from a polymer aqueous solution (0.05 wt %). The scale bar is 200 nm.

PVP-PA consisting of hydrophilic PVP and hydrophobic PA self-assembled in water. ^{1}H NMR spectra of PVP-PA (PIII) in CF_3COOD and in D_2O were compared (Figure 3). 3-(Trimethylsilyl)propanoic acid and tetramethylsilane were used as reference peaks of 0.0 ppm in D_2O and in CF_3COOD, respectively. The ^{1}H NMR peaks of PVP-PA (PIII) in CF_3COOD were 0.2−0.3 ppm downfield shifted from those in D_2O. This might result from the difference in the reference peaks, and hydrogen bonding between CF_3COOD and amide bonds of PVP and PA. In particular, the sharp methyl peak of PA (−NHCOCH(***CH_3***)−) at 1.5−1.8 ppm in CF_3COOD was significantly collapsed in D_2O whereas the methylene peak of PVP (-N***CH_2***CH_2CH_2CO−) at 3.3−3.8 ppm kept its shape. This behavior suggests that PVP-PAs form a core−shell structure in water where the hydrophilic PVPs form a shell and hydrophobic PAs form a core.[22,23]

The critical micelle concentration was determined by fluorescence spectroscopy. 2-Anilinonaphthalene shows fluorescence emission spectra at 350−600 nm. When the dye is located in a hydrophobic environment, an increase in the fluorescence intensity as well as a blue-shift of the fluorescence spectra occurs (Figure 4a).[26] Dye concentration was fixed at 10 μM and PVP-PA (PIII) concentration varied over 1.0×10^{-4}, 5.0×10^{-4}, 1.0×10^{-3}, 5.0×10^{-3}, 1.0×10^{-2}, 5.0×10^{-2}, 1.0×10^{-1}, and 5.0×10^{-1} wt %. The band position of the fluorescence spectra of the dye was plotted against logarithmic concentration to find the critical micelle concentration. The crossing point of the two extrapolated lines (insert in Figure 4a) was defined as the critical micelle concentration, which is about 0.01 wt %.

The micelle formation was also confirmed by transmission electron microscopy images. Spherical micelles in the range 30−90 nm were observed (Figure 4b). Even though there might have been some distortion during the water evaporation at 20 °C, the spherical micelles were clearly observed.

Dynamic light scattering study demonstrated the apparent size and size distribution of the polymer aggregates in water (Figure 5). The polymer aggregates of 20−70 nm in diameter at 20 °C are well-correlated with the size of micelles observed by the transmission electron microscopy image. On the other hand, the

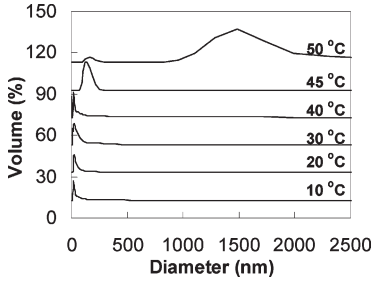

Figure 5. Apparent size distribution of PVP-PA (PIII) in water at 0.05 wt % as a function of temperature. The size was determined by dynamic light scattering. The aqueous solution was equilibrated for 20 min at each temperature.

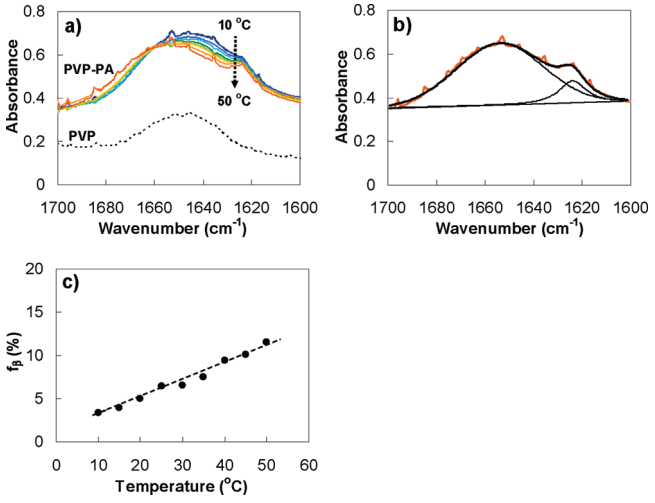

Figure 6. (a) FTIR spectra of PVP-PA (PIII) aqueous solution (12.0 wt % in D_2O) as a function of temperature by an increment of 5 °C from 10 to 50 °C. FTIR spectra of PVP-II aqueous solution (12.0 wt % in D_2O) at 20 °C was compared as a reference. (b) Deconvolution of the carbonyl peak (50 °C) by the XPSPEAK41 program. The orange line is the original carbonyl band at 50 °C and the thick black line is the simulated curve from the two deconvoluted peaks (black thin lines). (c) Replot of part a by the ratio (f_β) of a peak area centered at 1624 cm^{-1} to the whole carbonyl peak.

micelles abruptly increased to a size of 100 nm or larger with a broad distribution as the temperature increased to 45 °C. At the higher temperature of 50 °C, polymer aggregates larger than 1000 nm were observed, suggesting that the significant aggregation of polymers occurs at high temperature.[28]

To investigate the change in conformation of the PVP-PA on a molecular level, FTIR, CD, and ^{13}C NMR of the polymer aqueous solution were investigated as a function of temperature. Even though the carbonyl peak of the PVP homopolymer (PVP-II) overlapped the amide I band in FTIR spectra of PVP-PA aqueous solution (in D_2O), an increase in the shoulder peak centered at 1624 cm^{-1} was clearly observed as the temperature increased (Figure 6a). The FTIR peak at 1620−1630 cm^{-1} comes from the β-sheet structure of a polypeptide.[29−31] To analyze the increase in the peak centered at 1624 cm^{-1} in a semiquantitative manner, the carbonyl peak was deconvoluted into two peaks by the XPSPEAK41 program (Figure 6b). FTIR spectra of Figure 6a was replotted by the ratio of the area under the curve centered at 1624 cm^{-1} to the whole carbonyl peak of 1600−1700 cm^{-1} (Figure 6c). The ratio (f_β), a measure of the β-sheet structure, increased from 3% to 12% as the temperature increased from 10 to 50 °C. This fact suggests that the β-sheet structure of PA is partially strengthened as the temperature increases.

CD spectra of PVP-PA (PIII) aqueous solution were investigated as a function of the concentration and temperature.

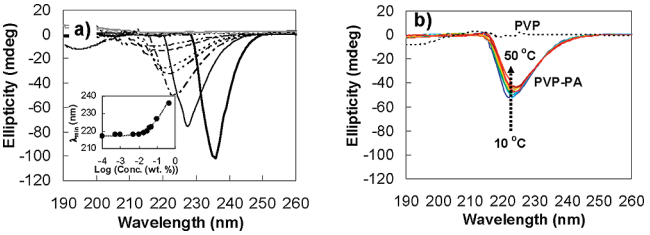

Figure 7. (a) CD spectra of PVP-PA (PIII) at 20 °C as a function of concentration. The polymer concentration varied over 1.0×10^{-4} to 5.0×10^{-1} wt %. (b) CD spectra of PVP-PA (PIII) at 0.05 wt % as a function of temperature by an increment of 5 °C from 10 to 50 °C. CD spectra of PVP-II aqueous solution (0.05 wt %) at 20 °C was compared as a reference.

Polymer concentration varied over 1.0×10^{-4}, 5.0×10^{-4}, 1.0×10^{-3}, 5.0×10^{-3}, 1.0×10^{-2}, 2.0×10^{-2}, 3.0×10^{-2}, 4.0×10^{-2}, 5.0×10^{-2}, 1.0×10^{-1}, and 5.0×10^{-1} wt % at a fixed temperature of 20 °C. As the polymer concentration increased above 0.01 wt %, a red-shift of a negative Cotton band from 218 to 236 nm was observed (Figure 7a). Such a red-shift of the negative Cotton band was also reported for poly(ethylene glycol)-poly(L-benzyl glutamate) (PEG-L-PBG) and poly(ethylene glycol)-poly(L-alanine) (PEG-L-PA) diblock copolymer aqueous solutions as the polymer concentration increased.[20,32] PEG did not develop any chiro-optical property, therefore, the self-assembly of the polypeptide with α-helixes or β-sheets was suggested for such a behavior. In our current study, PVP itself did not show any chiro-optical properties and the negative Cotton band came from the PA. Considering that FTIR spectra of PVP-PA partially developed a β-sheet structure in water, the negative Cotton band of PVP-PA came from the secondary structure of PA.[31,33,34] As the temperature increased at a fixed polymer concentration at 0.05 wt %, a small decrease in negative Cotton band centered at 222 nm was observed, suggesting a small change in the secondary structure of polypeptide (Figure 7b).

Based on the FTIR and CD spectra, we can conclude that the PAs of the PVP-PA form a mixed structure of random coils and β-sheets over the temperature range 10−50 °C, and the β-sheet conformation of PA is partially strengthened as the temperature increases.

^{13}C NMR spectra of PVP-PA aqueous solution (in D_2O) also showed a broadening and a downfield shift of the methylene peak of PVP (−NCH_2***CH_2***CH_2CO−) at 17−18 ppm and methyl peak of PA (−NHCOCH(***CH_3***)−) at 16−17 ppm (Figure 8) as the temperature increased to above the sol-to-gel transition temperature. The carbonyl peaks of PVP at 177−179 ppm and PA at 174−176 ppm showed a similar trend. The sol-to-gel transition of the PVP-PA aqueous solution decreased the molecular motion of both PVP and PA segments, resulting in the broadening and collapsing of the PVP and PA peaks in the ^{13}C NMR spectra.[35,36]

The structure−property relationship of sol−gel transition of the PVP-PA aqueous solution was studied by varying PA length, PVP length, and the composition of L-alanine/DL-alanine of the PA. As the hydrophobic PA block length increased, the sol-to-gel transition temperature decreased, suggesting that sol-to-gel transition is driven by hydrophobic association (Figure 9a). At the same PVP-PA concentration of 8.0 wt %, the sol-to-gel transition temperature of the PVP-PA decreased from 61 to 25 °C when the PA block length increased from 350 to 880 Da. In addition, f_β increased from 2.4 to 7.1 as the hydrophobic PA block length increased from 350 to 880 Da (Figure 9b).

As the hydrophilic PVP block length of PVP-PA decreased from 1240 to 970 Da, the sol-to-gel transition temperature significantly decreased (Figure 10a). Such a trend was also reported for polyester-based reverse thermogelling polymers.[37,38] Interestingly, f_β decreased from 6.7 to 2.6 as the hydrophilic PVP

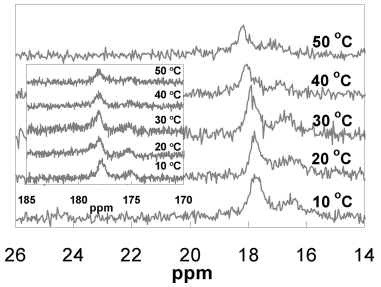

Figure 8. ^{13}C NMR spectra of the PVP-PA (PIII) in D_2O (12.0 wt %) as a function of temperature. Methyl peak of PA (−NHCOCH($\boldsymbol{CH_3}$)−) at 16.0−17.0 ppm and methylene peak of PVP (−$NCH_2\boldsymbol{CH_2}CH_2CO$−) at 17−18.3 ppm are shown. The carbonyl peaks of PA at 174.0−176.0 ppm and PVP at 177.0−179.0 ppm are compared as a function of temperature (insert).

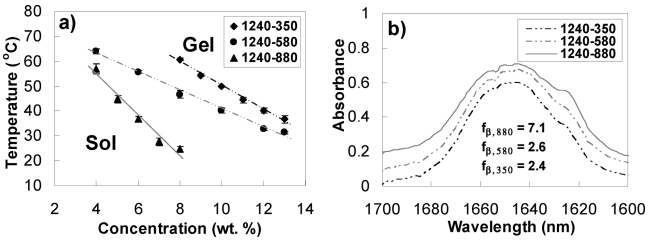

Figure 9. (a) Effect of the PA molecular weight on the phase diagram of the PVP-PA aqueous solution determined by the test tube inverting method (n = 3). (b) FTIR spectra of the PVP-PA aqueous solutions (12.0 wt % in D_2O). The ratio of L-alanine/DL-alanine is fixed at 30/70 and PVP molecular weight was fixed at 1240 Da. The legends are the molecular weight of each block. The molecular weight of PA is shown in f_β for simplicity.

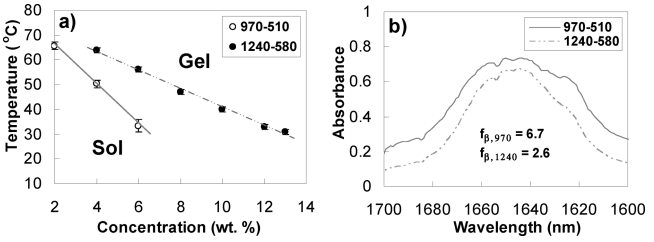

Figure 10. (a) Effect of the PVP molecular weight on the phase diagram of the PVP-PA aqueous solutions determined by the test tube inverting method (n = 3). (b) FTIR spectra of the PVP-PA aqueous solutions (12.0 wt % in D_2O). The ratio of L-alanine/DL-alanine is fixed at 30/70. The legends are molecular weight of each block. The molecular weight of PVP is shown in f_β for simplicity.

block length increased from 970 to 1240 Da (Figure 10b). The longer hydrophilic block might interfere more than the shorter hydrophilic block in the β-sheet packing of the polypeptide (PA) by steric hindrance.[39,40]

L-alanine/DL-alanine ratio of the PA varied over 20/80, 30/70, and 40/60 with a similar block length of PVP-PA. The ratio is assumed to be the same with the feed ratio of *N*-carboxy anhydrides of L-alanine to *N*-carboxy anhydrides of DL-alanine in the polymerization. As the composition of L-alanine increased, the sol-to-gel transition temperature decreased (Figure 11a). In addition, f_β increased from 2.2 to 4.9 as the composition of L-alanine increased (Figure 11b). As the composition of the stereoregular L-isomer increased, the polymer was effectively packed into a β-sheet structure, and the aggregation tendency of the polymer by hydrophobic association increased.[41] Therefore, the sol-to-gel transition temperature decreased as the composition of L-alanine of PA increased.

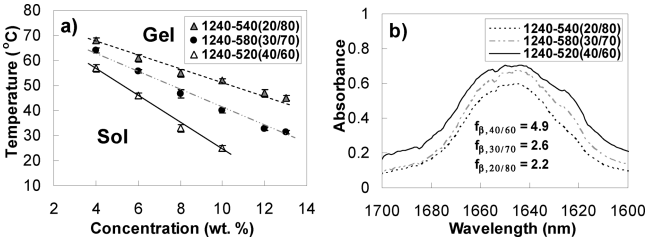

Figure 11. (a) Effect of the L-alanine/DL-alanine ratio of PA on the phase diagram of the PVP-PA aqueous solutions determined by the test tube inverting method (n = 3). (b) FTIR spectra of the PVP-PA aqueous solutions (12.0 wt % in D_2O). The molecular weight of PVP and PA were fixed at 1240 and 520−580 Da, respectively. The legends are the molecular weight of each block and L-alanine/DL-alanine ratio of PA. The L-alanine/DL-alanine ratio of PA is shown in f_β for simplicity.

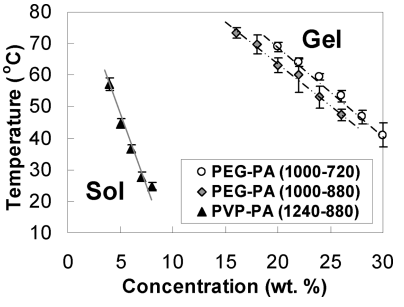

Figure 12. Comparison of phase diagram between PVP-PA and PEG-PA aqueous solutions. The ratio of L-alanine/DL-alanine is fixed at 30/70. The legends are the molecular weight of each block.

The structure−property relationship proved that the sol-to-gel transition temperature decreased as the hydrophobic PA block length increased, hydrophilic PVP length decreased, and the L-alanine/DL-alanine ratio increased. Such a trend also coincided with the tendency of β-sheet formation of the PA as shown by the change in f_β.

The sol-to-gel transition of the aqueous solutions of PVP-PA and PEG-PA with similar molecular weight and composition were compared (Figure 12). The molecular weight of the commercially available α-amino-ω-methoxy PEG is limited, and thus a molecular weight of 1000 Da was used to prepare the PEG-PA. The ratio of L-Ala to DL-Ala was fixed at 30/70 to keep consistence with corresponding PVP-PA in current study. The MALDI−TOF mass spectra and ^1H NMR spectra of the PEG-PA are shown in Supporting Information (Figure S2 and Figure S3). As shown in Figure 10, an increase in the molecular weight of hydrophilic block increases the sol-to-gel transition temperature of the amphiphilic polymer aqueous solution, and increases the concentration ranges that show sol-to-gel transition.[9] Even though the PVP-PA (1240−880) diblock copolymer has a higher molecular weight of the hydrophilic block than the PEG-PA (1000−880) diblock copolymer, the sol-to-gel transition of PVP-PA aqueous solutions occurred at lower concentrations than PEG-PA. At a similar ratio of hydrophobic block to hydrophilic block, PVP-PA (1240−880) and PEG-PA (1000−720) could be compared. The ratios are 0.71 and 0.72, respectively. The sol-to-gel transition temperatures of PVP-PA aqueous solutions were lower than those of PEG-PA. Therefore, PEG seems to act significantly more hydrophilic than PVP in driving the sol-to-gel transition of a corresponding amphiphilic block copolymer.

PVP-PA (PIII) has a powder form at room temperature, which is thus convenient to handle and weigh, whereas above PEG-PAs has a rather sticky morphology at room temperature. In particular, the dissolution time of PVP-PA (PIII) was about 20 min, whereas that of previous poly(ethylene glycol)−polyalanine

(PEG-PA) or poly(ethylene glycol)−poly(alanine-*co*-phenylalanine) (PEG-PAF) took one to several hours to prepare an aqueous solution (1.0 mL) that underwent sol-to-gel transition.[18,20] The characteristics of the powder morphology and the short dissolution time of the PVP-PA in water indicate that the reconstitution of a drug formulation can be facilitated.

An in situ formed PVP-PA gel prepared from an aqueous polymer (PIII) solution (0.5 mL; 12.0 wt %) was tested for its stability. Phosphate buffered saline (3.0 mL) at 37 °C was added on top of the gel and the whole medium (3.0 mL) was replaced daily.[18] In vitro study showed that the PVP-PA (PIII) gel prepared from an polymer aqueous solution (12.0 wt %) decreased by less than 10% over two weeks, suggesting that it is practically intact in water. A Pluronic F127 ((ethylene glycol)$_{99}$-(propylene glycol)$_{65}$-(ethylene glycol)$_{99}$) triblock copolymer hydrogel prepared from an initial polymer concentration of 30.0 wt% completely disappeared within 5 days by the same protocol.

Conclusions

To conclude, a reverse thermogelling PVP-PA aqueous solution has been developed. The amphiphilic polymers consisting of hydrophilic PVP and hydrophobic PA blocks form micelles in water. To investigate the mechanism and structure property relationship of sol-to-gel transition, a series of PVP-PAs undergoing reverse thermal gelation were synthesized. CD, FTIR, and ^{13}C NMR spectra suggest that the sol-to-gel transition is driven by hydrophobic association and accompanies a slight increase in β-sheet structure. As an alternative to PEG, the PVP could be a promising hydrophilic polymer in designing a new biomaterial.

Acknowledgment. This work was supported by the Korea Research Foundation (Grant No. KRF-2008-313-C00590), and Korea Science and Engineering Foundation (KOSEF) grants funded by the Korean government (MEST;Grant Nos. 2009-0080447 and R11-2005-008-00000-0).

Supporting Information Available: Figures showing ^{1}H NMR spectra of PVP-PA (PIII) and PEG-PA (in CF_3COOD) and MALDI−TOF mass spectra of PEG-PA. This material is available free of charge via the Internet at http://pubs.acs.org.

References and Notes

(1) Appel, W.; Biekert, E. *Angew. Chem., Int. Ed.* **1968**, *7*, 702–708.
(2) Kamada, H.; Tsutsumi, Y.; Tsunoda, S.; Kihira, T.; Kaneda, Y.; Yamamoto, Y.; Nakagawa, S.; Horissawa, Y.; Mayumi, T. *Biochem. Biophys. Res. Commun.* **1999**, *257*, 448–453.
(3) Torchilin, V. P.; Shtilman, M. I.; Trubetskoy, V. S.; Whiteman, K.; Milstein, A. M. *Biochim. Biophys. Acta* **1994**, *1195*, 181–184.
(4) Benahmed, A.; Leroux, J.-C. *Pharm. Res.* **2001**, *18*, 323–328. (b) Lukyanov, A. N.; Torchilin, V. P. *Adv. Drug Delivery Rev.* **2004**, *56*, 1273–1289. (c) Lou, L.; Ranger, M.; Lessard, D.; Le Garrec, D.; Gori, S.; Leroux, J.-C.; Rimmer, S.; Smith, D. *Macromolecules* **2004**, *37*, 4008–4013. (d) Le Garrec, D.; Gori, S.; Luo, L.; Lessard, D.; Smith, D. C.; Yessine, M.-A.; Ranger, M.; Leroux, J.-C. *J. Controlled Release* **2004**, *99*, 83–101. (e) Chung, T. W.; Cho, K. Y.; Lee, H.-C.; Nah, J. W.; Yeo, J. H.; Akaike, T.; Cho, C. S. *Polymer* **2004**, *45*, 1591–1597. (f) Bartolozzi, I.; Solaro, R.; Schacht, E.; Chiellini, E. *Eur. Polym. J.* **2007**, *43*, 4628–4638.
(5) Park, I. K.; Ihm, J. E.; Park, Y. H.; Choi, Y. J.; Kim, S. I.; Kim, W. J.; Akaike.; Cho, C. S. *J. Controlled Release* **2003**, *86*, 349–359.
(6) Gaucher, G.; Asahina, K.; Wang, J.; Leroux, J.-C. *Biomacromolecules* **2009**, *10*, 408–416.
(7) Doebbler, G. F. *Cryobiology* **1966**, *3*, 2–11.
(8) Townsend, M. W.; Deluca, P. P. *J. Parenter. Sci. Technol.* **1988**, *42*, 190–199.
(9) Joo, M. K.; Park, M. H.; Choi, B. G.; Jeong, B. *J. Mater. Chem.* **2009**, in press, DOI: 10.1039/b902208b
(10) Yu, L.; Ding, J. *Chem. Soc. Rev.* **2008**, *37*, 1473–1481.
(11) Nagahama, K.; Ouchi, T.; Ohya, Y. *Adv. Funct. Mater.* **2008**, *18*, 1220–1231.
(12) Jeong, B.; Bae, Y. H.; Kim, S. W. *Macromolecules* **1999**, *32*, 7064–7069.
(13) Chenite, A.; Chaput, C.; Wang, D.; Combes, C.; Buschmann, M. D.; Hoemann, C. D.; Leroux, J. C.; Atkinson, B. L.; Binette, F.; Selmani, A. *Biomaterials* **2000**, *21*, 2155–2161.
(14) Lee, B. H.; Lee, Y. M.; Sohn, Y. S.; Song, S. C. *Macromolecules* **2002**, *35*, 3876–3879.
(15) Vermonden, T.; Besseling, N. A. M.; Van Steenbergen, M. J.; Hennink, W. E. *Langmuir* **2006**, *22*, 10180–10184.
(16) Kim, S. Y.; Kim, H. J.; Lee, K. E.; Han, S. S.; Sohn, Y. S.; Jeong, B. *Macromolecules* **2007**, *40*, 5519–5525.
(17) Choi, B. G.; Sohn, Y. S.; Jeong, B. *J. Phys. Chem. B.* **2007**, *111*, 7715–7718.
(18) Jeong, Y.; Joo, M. K.; Bahk, K. H.; Choi, Y. Y.; Kim, H. T.; Kim, W. K.; Sohn, Y. S.; Jeong, B. *J. Controlled Release* **2009**, *137*, 25–30.
(19) Wright, E. R.; Conticello, V. P. *Adv. Drug. Deliv. Rev.* **2002**, *54*, 1057–1073.
(20) Choi, Y. Y.; Joo, M. K.; Sohn, Y. S.; Jeong, B. *Soft Matter* **2008**, *4*, 2383–2387.
(21) Lecommandoux, S.; Achard, M. F.; Langenwalter, J. F.; Klok, H. A. *Macromolecules* **2001**, *34*, 9100–9111.
(22) Jun, Y. J.; Toti, U. S.; Kim, H. Y.; Yu, J. Y.; Jeong, B.; Jun, M. J.; Sohn, Y. S. *Angew. Chem., Int. Ed.* **2006**, *45*, 6173–6176.
(23) Chen, C.; Yua, C. H.; Cheng, Y. C.; Yua, P. H. F.; Cheung, M. K. *Biomaterials* **2006**, *27*, 4804–4814.
(24) Tanodekaew, S.; Godward, J.; Heatley, F.; Booth, C. *Macromol. Chem. Phys.* **1997**, *198*, 3385–3395.
(25) Nystrolm, B.; Walderhaug, H. *J. Phys. Chem.* **1996**, *100*, 5433–5439.
(26) Arotcarena, M.; Heise, B.; Ishaya, S.; Laschewsky, A. *J. Am. Chem. Soc.* **2002**, *124*, 3787–3793.
(27) Jin, S.; Liu, M.; Chen, S.; Gao, C. *Eur. Polym. J.* **2008**, *44*, 2162–2170.
(28) Park, S. H.; Choi, B. G.; Joo, M. K.; Han, D. K.; Sohn, Y. S.; Jeong, B. *Macromolecules* **2008**, *41*, 6486–6492.
(29) Yamada, N.; Ariga, K.; Natio, M.; Matsubara, K.; Koyama, E. *J. Am. Chem. Soc.* **1998**, *120*, 12192–12199.
(30) Baginska, K.; Makowska, J.; Wiczk, W.; Kasprzykowski, F.; Chmurzynski, L. *J. Peptide Sci.* **2008**, *14*, 283–289.
(31) Oh, H. J.; Joo, M. K.; Sohn, Y. S.; Jeong, B. *Macromolecules* **2008**, *41*, 8204–8209.
(32) Ding, W.; Lin, S.; Lin, J.; Zhang, L. *J. Phys. Chem. B* **2008**, *112*, 776–783.
(33) Hwang, J.; Deming, T. J. *Biomacromolecules* **2001**, *2*, 17–21.
(34) Hamley, I. W.; Ansari, I. A.; Castelletto, V.; Nuhn, H.; Rosler, A.; Klok, H. A. *Biomacromolecules* **2005**, *6*, 1310–1315.
(35) Yu, L.; Zhang, H.; Ding, J. *Angew. Chem., Int. Ed.* **2006**, *45*, 2232–2235.
(36) Yang, C.; Ni, X.; Li, J. *J. Mater. Chem.* **2009**, DOI: 10.1039/b900198k, in press.
(37) Hwang, M. J.; Suh, J. M.; Bae, Y. H.; Kim, S. W.; Jeong, B. *Biomacromolecules* **2005**, *6*, 885–890.
(38) Bae, S. J.; Joo, M. K.; Jeong, Y.; Kim, S. W.; Lee, W. K.; Sohn, Y. S.; Jeong, B. *Macromolecules* **2006**, *39*, 4873–4879.
(39) Lim, Y B.; Lee, M. *J. Mater. Chem.* **2008**, *18*, 723–727.
(40) Choi, Y. Y.; Jeong, Y.; Joo, M. K.; Jeong, B. *Macromol. Biosci.* **2009**, DOI:10.1002/mabi.200900095, in press.
(41) Joo, M. K.; Sohn, Y. S.; Jeong, B. *Macromolecules* **2007**, *40*, 5111–5115.